Toward High-speed Transcranial Photoacoustic Imaging using Compact Near-infrared Pulsed LED Illumination System

Jeeun Kang[a], Haichong Kai Zhang[a], Alexis Cheng[a], Arman Rahmim[a,c], Dean F. Wong[a], Jin U. Kang[c], and Emad M. Boctor* [a,b,c]

[a]Laboratory for Computational Sensing and Robotics, Whiting School of Engineering, Johns Hopkins University, Baltimore, MD, USA; [b]Department of Radiology, School of Medicine, Johns Hopkins University, Baltimore, MD, USA; [c]Department of Electrical & Computer Engineering, School of Medicine, Johns Hopkins University, Baltimore, MD, USA

ABSTRACT

Quantification of brain function is a significant milestone towards understanding of the underlying workings of the brain. Photoacoustic (PA) imaging is the emerging brain sensing modality by which the molecular light absorptive contrast can be non-invasively quantified from deep-lying tissue (~several cm). In this BRAIN initiative effort, we propose high-speed transcranial PA imaging using a novel, compact pulsed LED illumination system (Prexion Inc., Japan) with 200-uJ pulse energy for 75-ns duration, and pulse repetition frequency (PRF) up to 4kHz at near-infrared (NIR) wavelengths of 690-nm and 850-nm switchable in real-time. To validate the efficacy of the proposed system, preliminary ex vivo experiments were conducted with mice skull and human temporal bone, which included vessel-mimicking tubes filled with 10% Indian Ink solution and light absorptive rubber material, respectively. The results indicated that significant PA contrast, 150% signal-to-noise ratio (SNR), can be achieved through the mice skull only with 64 subsequent frame averaging. The minimal number of frames for averaging required was only 16 to generate signal above background noise, leading to 250 Hz frame rate in the strictest temporal frame separation. Furthermore, distinguishable PA contrast was achieved with human temporal bone with 64-frame averaging. Overall, the preliminary results indicate that the LED illumination system can be a cost-effective solution for high-speed PA brain imaging in preclinical and clinical applications, compared to expansive and bulky Nd:YAG laser systems commonly used in PA imaging.

Keywords: photoacoustics, non-invasive transcranial brain imaging, LED light source, near-infrared, high-speed

Corresponding author, E-mail: eboctor1@jhmi.edu

1. INTRODUCTION

The quantification and monitoring of brain function have been desired as a significant milestone toward understanding of the underlying workings of the brain representing its internal functionality or responses to external stimulation. For conventional non-invasive sensing, PET and MRI is used, but they have their own disadvantages to monitor the brain activities; PET can provide high pharmacological specificity, but it suffers from low temporal resolution. Otherwise, MRI can provide higher spatial and temporal resolution. However, it provides low specificity for brain activities. On the other hand, there have been optical imaging approaches of a brain, but they have small dynamic range and only shallow penetration depth due to light scattering and absorbance during penetration into intact skull *in vivo*.

In biomedical diagnostic field, photoacoustic (PA) imaging have been highlighted as a novel hybrid modality which can provide the molecular contrast of light absorbance with sufficient acoustic penetration depth (~several cm) and spatial resolution (e.g., 800 um). In PA imaging, radio-frequency (RF) acoustic pressure is generated depending on the light absorbance and thermo-elastic property of a target when the light energy at specific wavelength is delivered to a target. The generated acoustic pressure propagates the biological tissue, and obtained by ultrasound transducer. Using the physical mechanism, there have been broad configurations for biomedical applications; microscopic configuration basically employs the high-speed laser source at low amount of energy (~μJ), which scanning the surface of a target with

Photons Plus Ultrasound: Imaging and Sensing 2017, edited by Alexander A. Oraevsky, Lihong V. Wang, Proc. of SPIE Vol. 10064, 100643B · © 2017 SPIE · CCC code: 1605-7422/17/$18 · doi: 10.1117/12.2253322

Downloaded From: https://www.spiedigitallibrary.org/conference-proceedings-of-spie on 8/28/2017 Terms of Use: https://spiedigitallibrary.spie.org/ss/TermsOfUse.aspx

focused configuration of light and acoustics. By doing so, the optical spatial resolution microscopy (~several nm) can be constructed for biomedical applications such as single cell imaging [1], melanoma detection [2], and eye imaging [3]. However, the microscopic approach only yield limited imaging depth up to several mm. Otherwise, there are attempts to yield deeper imaging depth (~several cm) by integrating clinical ultrasound imaging machine and high-power pulsed light source. The configuration can construct the hybrid imaging mode between ultrasound and PA images so that the anatomic and molecular information can both be provided. Using the configuration, various applications are being researched; sentinel lymph node detection for screening cancer metastasis [4], breast microcalcifications detection for early-detection of breast cancer [5-7], tissue characterization for thyroid and ovarian tumor lesion [8,9], etc. The imaging dimension can be further extended using tomographic configuration. The light can be delivered in diffusive manner, and the PA signal can be collected the multiple sensors surrounding the target being imaged. Using the deep penetrating capability, there have been several researches to image a brain of rodent to non-human primate animals; mice brain imaging [10], functional connectivity mapping in the mouse brain. [11] Particularly, Xinmai Yang, et al. and Chao Huang presented the PA imaging is capable of imaging a monkey brain in transcranial imaging using high-power pulsed laser illumination at 1064 and 630 nm, respectively. [12,13] For both cross-sectional and tomographic imaging configuration, high-power tunable illumination systems such as optical parametric oscillator (OPO)-integrated Nd:YAG or dye lasers are usually used to obtain deep penetration depth for biological tissue. However, they used Nd:YAG-based laser system whose pulse repetition frequency (PRF) is limited to 10 Hz to ensure the light penetration into intact skull.

In this BRAIN initiative effort, we propose new approach for high-speed transcranial PA imaging of cerebral cortex covering the superficial region of brain by using a novel, compact pulsed LED illumination system (NIR-LED) (Prexion Inc., Japan) which can provide 200-uJ pulse energy for 75-ns duration, and pulse repetition frequency (PRF) up to 4kHz at near-infrared (NIR) wavelengths.

2. METHOD

2.1 Experimental setup

The PA sensing system was employed for evaluating the proposed LED-based PA imaging performance; A near-infrared pulsed LED illumination system (Prexion Inc., Japan) was used for PA signal generation. Table 1 summarizes the specifications of the compact and safe laser system; The arrays of HDHP LED light source can be comprised by various wavelengths throughout 365 to 1450 nm. Especially, near-infrared wavelengths such as 690, 760, 780, 850 nm can be used for diagnostic PA imaging with deep penetration depth. Also, the system supports combination mode between 690 and 850 nm. The effective illumination area of each LED head is 50 x 7 mm^2 which is compatible for common clinical ultrasound array transducer. The pulse energy is up to 200 μJ at variable pulse width from 30 – 135 nm. The pulse repetition rate is up to 4 kHz, which is desirable for high-speed PA imaging. To collect the generated PA signals, ultrasound research package with data acquisition system (SonixTouch and SonixDAQ, Ultrasonix Corp., Canada) was used with a 10-MHz linear ultrasound probe (L14-5/38, Ultrasonix Corp.).

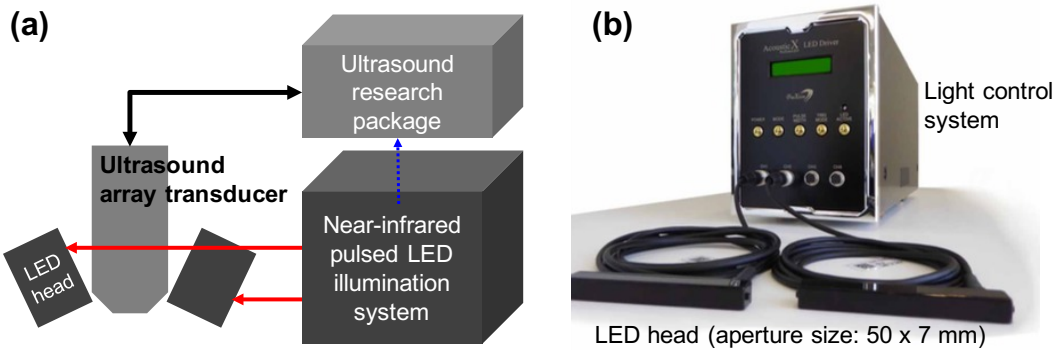

Figure 1 Preliminary experimental setup: (a) system configuration, (b) near-infrared pulsed LED illumination system

Downloaded From: https://www.spiedigitallibrary.org/conference-proceedings-of-spie on 8/28/2017 Terms of Use: https://spiedigitallibrary.spie.org/ss/TermsOfUse.aspx

Table 1. Specifications of the near-infrared, pulsed LED illumination system

	Specifications
Light source	HDHP LED
Maximum energy per pulse	850 nm: 200 μJ/pulse 690 nm: 80 μJ/pulse 925 nm: 80 μJ/pulse
Wavelength	365, 405, 525, 630, 690, 760, 780, 850, 930, 1050, 1200, 1450 nm (single mode), 690/850 nm (combination mode)
Effective illumination area	50 x 7 mm^2
PRF	Variable up to 4kHz
Pulse width	Selectable from 30, 45, 60, 75, 90, 105, 120, 135 nm
Driver ports	4
Pulse trigger mode	Normal or alternate drive mode for combination LED setup
Pulse trigger ports	Internal trigger output x 1 External trigger input x 1

2.2 Sample preparation

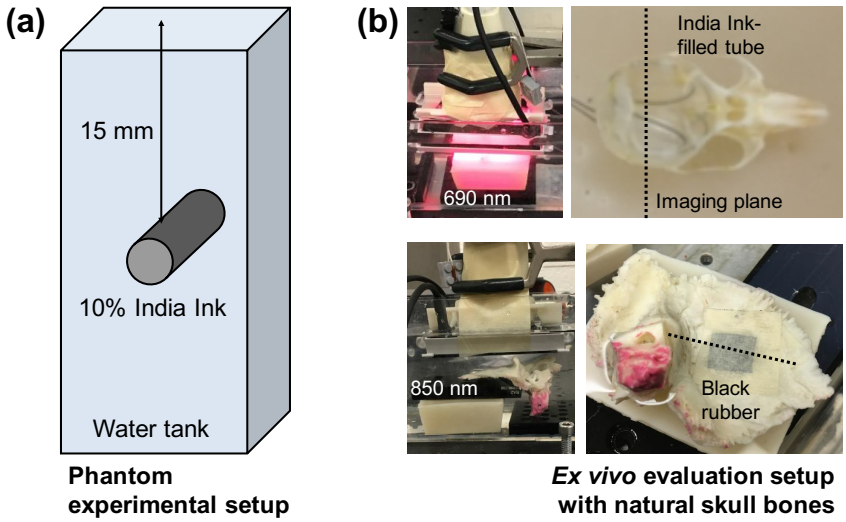

Figure 2 *Ex vivo* transcranial photoacoustic imaging setup using near-infrared pulsed LED illumination system: (a) phantom experimental setup at 850 nm, (b) mice skull imaging at 690 nm, human temporal bone imaging at 850 nm, respectively.

To evaluate the performance of PA imaging system based on NIR-LED system, phantom and *ex vivo* sample were prepared as show in Figure 2; The phantom experiment in Figure 2a was designed to quantify the signal-to-noise ratio enhancement depending on the number of averaged frame, which can take full advantage of high pulse repetition rate up to 4 kHz. The 10% India Ink solution was loaded into transparent tubes with 1.27-mm diameter (AAQ04133, Tygon®

Downloaded From: https://www.spiedigitallibrary.org/conference-proceedings-of-spie on 8/28/2017 Terms of Use: https://spiedigitallibrary.spie.org/ss/TermsOfUse.aspx

Medical Tubing, Saint-Gobain Corp.), which were located at around 15 mm depth in the water tank. Note that the temperature of the water was consistently maintained at 22ºC during the experiments. The signal-to-noise ratio (SNR) was quantified as follows:

$$SNR = 10\log_{10}\frac{I_{signal}}{I_{noise}} \quad (1)$$

The identical imaging setup was applied to the PA imaging experiments with *ex vivo* skull samples as shown in Figure 2b; The thin Tygon tubing with 0.51-mm diameter (AAQ04103) filled with India Ink was injected into the whole mice skull as shown in Figure 1a. The PA signal was generated using 690-nm LED source, and collected thought the skull. Also, the human temporal bone was also used for preliminary feasibility test. The black rubber material was attached behind the skull sample and imaged with 850 nm LED heads.

3. RESULTS

3.1 Phantom experiments

Figure 3 shows the phantom experimental results to quantify the SNR according to the different number of frame averaging. Figure 3a present the PA images at 16 and 1000 frame averaging at 850 nm. In visual assessment, the 16 frame-averaging only produce low contrast compared to the background noise, while 1000 frame averaging yield significant contrast for the India Ink-filled tygon tube. For quantitative evaluation of SNR per the number of frame averaging, Figure 3b was constructed by calculating SNR for each frame averaging setup (i.e., 1, 4, 16, 32, 64, 128, 200, 300, 500, 1000) with the regions-of-interest indicated in Figure 3a. As shown in the figure, the SNR is proportional to the square root of number of averaged frames, and noise-equivalent sensitivity was acquired when 4 frames were utilized for averaging.

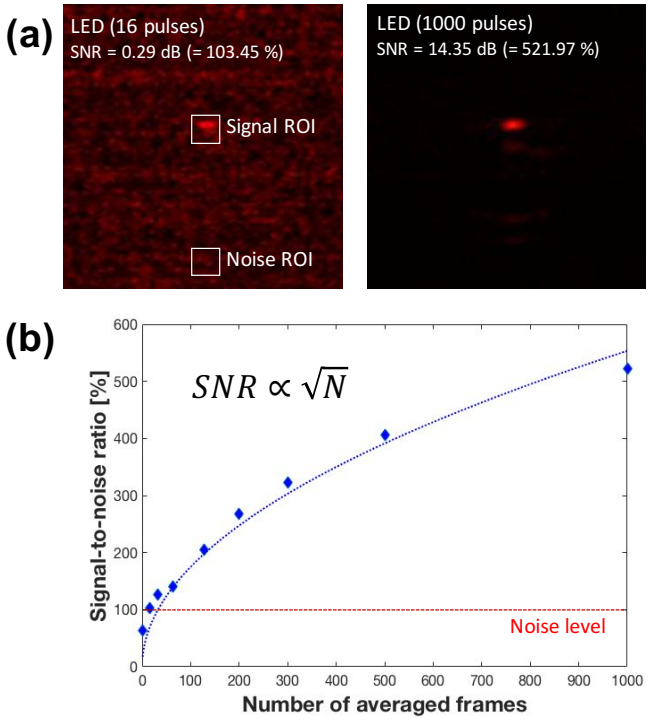

Figure 3 Phantom experimental results; (a) photoacoustic images at different number of frames for temporal averaging (i.e., 16 vs. 1,000), (b) signal-to-noise ratio versus number of averaged frames

Downloaded From: https://www.spiedigitallibrary.org/conference-proceedings-of-spie on 8/28/2017 Terms of Use: https://spiedigitallibrary.spie.org/ss/TermsOfUse.aspx

3.2 *Ex vivo* experiments

Ex vivo experimental results are presented in Figure 4. Figure 4a shows the transcranial PA imaging through the mice skull. Since two Tygon tubing was posed right behind the skull surface as shown in Figure 2b, two adjacent PA signals was clearly identified compared to the background. Figure 4b also shows the PA signals acquired through human temporal bone. Despite of thicker skull layer than that of mice, the PA signal generated from an absorptive target was clearly differentiated from the background.

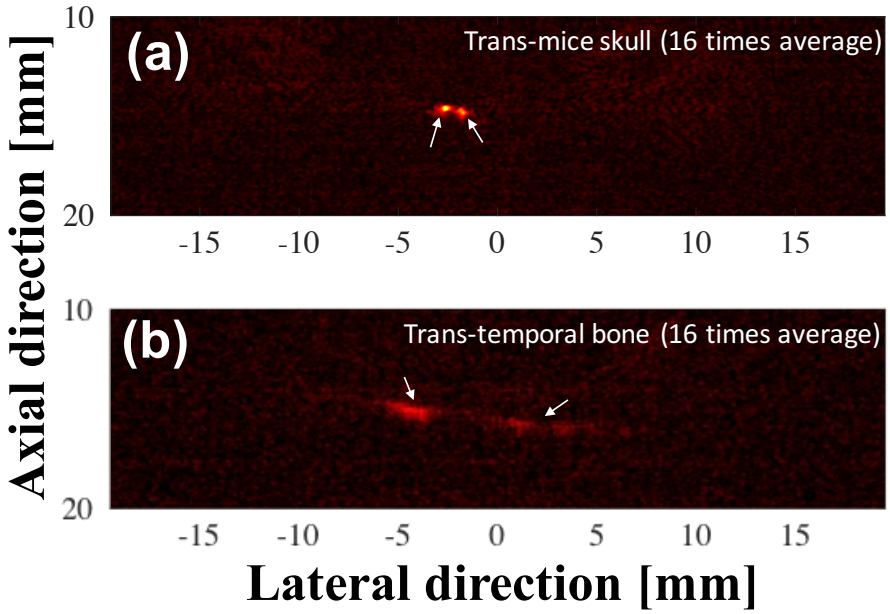

Figure 4 Preliminary *ex vivo* photoacoustic imaging results for (a) mice and (b) human skull samples.

4. DISCUSSION AND CONCLUSION

In this paper, we present the preliminary results of non-invasive transcranial PA imaging using a near-infrared pulsed LED illumination systems. In phantom experiments, the SNR according to different frame averaging setup was evaluated. The proposed PA imaging based on NIR-LED system produce the proportional SNR increase to the square root of the number of averaged frames. In *ex vivo* experiments using mice and human skull bones, the India Ink and black rubber were used as an absorptive materials. The NIR-LED-based PA imaging clearly differentiated the PA signals through the skull samples. However, further studies should be conducted to guarantee the efficacy of NIR-LED system in clinical applications; Clinical feasibility should be detailed in transcranial brain imaging based on endogenous and exogenous contrast agents. The hemoglobin is known as the strongest endogenous absorber within human body. The proposed PA sensing system based on the near-infrared pulsed LED illumination system can potentially obtain the blood oxygen level dependent (BOLD) contrast as previously proposed with high-power laser systems. To validate the feasibility of PA sensing based on NIR-LED should be validated with the whole blood sample. For this, *ex vivo* experimental evaluation conducted in this paper can be repeated by simply alternating the India Ink to the whole blood sample. Otherwise, the voltage sensitive dye (VSD) imaging can be used as an exogenous contrast agent for sensing brain functionality non-invasively using the proposed PA imaging system. To ensure the VSD sensitivity in transcranial brain imaging, the near-infrared wavelengths should be used. The feasibility test would be conducted to validate the advantages of NIR-LED which supports near-infrared wavelengths such as 690, 760, 780, 850 nm. Another important

Downloaded From: https://www.spiedigitallibrary.org/conference-proceedings-of-spie on 8/28/2017 Terms of Use: https://spiedigitallibrary.spie.org/ss/TermsOfUse.aspx

issue is enhancement of penetration depth of light energy generated by NIR-LED system. While NIR-LED can produce 200-uJ pulse with up to 4-kHz PRF, which can yield decent amount of PA signals. However, since it is still lower than that of the high-power laser such as Nd:YAG or dye lasers about 50-times, so that the sensitivity should be more enhanced using advanced signal processing algorithms. For example, coded excitation and compression method can be employed. For example, previous researches presented the periodic and unipolar code sequence can improve the SNR up to around 25 dB. [14]

ACKNOWLEDGEMENT

The financial supports were provided by NIH Brain Initiative grant, R24MH106083-03 and NIH grant R01EB01963.

REFERENCES

[1] Strohm, E.M., Berndl, E.S.L., and Kolios, M.C., "High frequency label-free photoacoustic microscopy of single cells," Photoacoustics 1(3-4), 49–53 (2013).

[2] Zhang, H.F., Maslov, K., Stoica, G., and Wang, L.V., "Functional photoacoustic microscopy for high-resolution and noninvasive in vivo imaging.," Nature Biotechnology 24(7), 848–851 (2006).

[3] la Zerda, de, A., Paulus, Y.M., Teed, R., Bodapati, S., Dollberg, Y., Khuri-Yakub, B.T., Blumenkranz, M.S., Moshfeghi, D.M., and Gambhir, S.S., "Photoacoustic ocular imaging," Optics Letters 35(3), 270–272 (2010).

[4] Garcia-Uribe, A., Erpelding, T.N., Krumholz, A., Ke, H., Maslov, K., Appleton, C., Margenthaler, J.A., and Wang, L.V., "Dual-Modality Photoacoustic and Ultrasound Imaging System for Noninvasive Sentinel Lymph Node Detection in Patients with Breast Cancer," Scientific reports 5, 15748 (2015).

[5] Kang, J., Kim, E.-K., Kim, G.R., Yoon, C., Song, T.-K., and Chang, J.H., "Photoacoustic imaging of breast microcalcifications: a validation study with 3-dimensional ex vivo data and spectrophotometric measurement.," Journal of Biophotonics 8(1-2), 71–80 (2015).

[6] Kim, G.R., Kang, J., Kwak, J.Y., Chang, J.H., Kim, S.I., Youk, J.H., Moon, H.J., Kim, M.J., and Kim, E.-K., "Photoacoustic imaging of breast microcalcifications: a preliminary study with 8-gauge core-biopsied breast specimens.," PLoS ONE 9(8), e105878 (2014).

[7] Kang, J., Kim, E.-K., Young Kwak, J., Yoo, Y., Song, T.-K., and Ho Chang, J., "Optimal laser wavelength for photoacoustic imaging of breast microcalcifications," Applied Physics Letters 99(15), 153702 (2011).

[8] Kang, J., Chung, W.Y., Kang, S.-W., Kwon, H.J., Yoo, J., Kim, E.-K., Chang, J.H., Song, T.-K., Lee, S., et al., "Ex Vivo Estimation of Photoacoustic Imaging for Detecting Thyroid Microcalcifications," PLoS ONE 9(11), (2014).

[9] Salehi, H.S., Li, H., Merkulov, A., Kumavor, P.D., Vavadi, H., Sanders, M., Kueck, A., Brewer, M.A., and Zhu, Q., "Coregistered photoacoustic and ultrasound imaging and classification of ovarian cancer: ex vivo and in vivo studies.," Journal of Biomedical Optics 21(4), 46006–12 (2016).

[10] Wang, L.V., and Hu, S., "Photoacoustic tomography: in vivo imaging from organelles to organs.," Science 335(6075), 1458–1462 (2012).

[11] Nasiriavanaki, M., Xia, J., Wan, H., Bauer, A.Q., Culver, J.P., and Wang, L.V., "High-resolution photoacoustic tomography of resting-state functional connectivity in the mouse brain," Proceedings of the National Academy of Sciences of the United States of America 111(1), 21–26 (2014).

[12] Yang, X., and Wang, L.V., "Monkey brain cortex imaging by photoacoustic tomography," Journal of Biomedical Optics 13(4), 044009–5 (2008).

[13] Huang, C., Nie, L., Schoonover, R.W., Guo, Z., Schirra, C.O., Anastasio, M.A., and Wang, L.V., "Aberration correction for transcranial photoacoustic tomography of primates employing adjunct image data," Journal of Biomedical Optics 17(6), 0660161–0660168 (2012).

[14] Zhang, H.K., Kondo, K., Yamakawa, M., and Shiina, T., "Coded excitation using periodic and unipolar M-sequences for photoacoustic imaging and flow measurement," Optics Express 24(1), 17–29 (2016).

Downloaded From: https://www.spiedigitallibrary.org/conference-proceedings-of-spie on 8/28/2017 Terms of Use: https://spiedigitallibrary.spie.org/ss/TermsOfUse.aspx